Optical and morphological properties of ZnO and Alq3 incorporated polymeric thin layers fabricated by the dip-coating method

M. Sypniewska, R. Szczesny, L. Skowronski, P. Kamedulski, E. Gondek, Aleksandra Apostoluk, B. Derkowska-Zielinska

Applied Nanoscience (2023) 13:4903–4912
https://doi.org/10.1007/s13204-022-02647-8

ORIGINAL ARTICLE

Optical and morphological properties of ZnO and Alq_3 incorporated polymeric thin layers fabricated by the dip-coating method

M. Sypniewska[1] · R. Szczesny[2] · L. Skowronski[3] · P. Kamedulski[2,4] · E. Gondek[5] · A. Apostoluk[6] · B. Derkowska-Zielinska[1]

Received: 21 February 2022 / Accepted: 21 September 2022 / Published online: 17 October 2022

Abstract

In this report, we present the influence of polymer matrix on morphological and optical properties of thin films containing zinc oxide (ZnO), tris(8-hydroxyquinolinato)aluminium (Alq_3) and ZnO:Alq_3. Polyvinylpyrrolidone (PVP) and poly(methyl methacrylate) (PMMA) dissolved in isopropanol and tetrahydrofuran, respectively, were used as polymeric matrices of fabricated composites. The analysed thin layers were deposited on Si substrates using a dip-coating method and characterized by Fourier-Transform Infrared Spectroscopy (FTIR), Energy-Dispersive X-ray spectroscopy (EDX), Atomic Force Microscopy (AFM), Scanning Electron Microscopy (SEM), Spectroscopic Ellipsometry (SE) and photoluminescence (PL). It was found that adding the polymer to Alq_3 causes a blueshift in absorption compared to pure Alq_3 layers. We also observed photoluminescence in the region of 2.2–2.8 eV for ZnO:Alq_3:PMMA and ZnO:Alq_3:PVP, as well as for Alq_3:PMMA at room temperature. PL measurements showed that adding ZnO to Alq_3:polymer matrix did not result in any shift in PL spectra compared to the results of Alq_3:polymer layer. AFM and SEM measurements show that relatively smooth films were obtained in the case of composites based on PVP and PMMA. Moreover, a change in the size of ZnO agglomerates depending on polymer used is observed for the three-component layers. We also noticed that the values of the refractive index are higher for the samples in the PVP matrix. However, the opposite behaviour was observed in the case of the extinction coefficient.

Keywords Zinc oxide · Tris(8-hydroxyquinolinato)aluminium · PVP · PMMA · Physico-chemical properties · Spectroscopic ellipsometry · Photoluminescence

Introduction

In recent years, inorganic/organic hybrid materials have attracted more and more interest, as even though individual materials have distinct physical or chemical properties, the final new composite, instead of adding the properties of the two materials, can show improved properties or entirely new ones (Yoshida et al. 2009; Boeckler et al. 2007; Sanchez et al. 2005). The combination of organic/inorganic hybrid materials provides better transport properties of charge carriers, which offers excellent potential for improving the parameters of optoelectronic devices (Onlaor et al. 2012; Coe et al. 2002).

Tris(8-hydroxyquinolinato)aluminium (Alq_3) is one of the most widely studied organometallic compounds due to its interesting properties and potential applications in optoelectronics. It exhibits features similar to inorganic semiconductors, i.e. relative stability, simple synthesis and good electronic transport (Cuba and Muralidharan 2014a;

✉ B. Derkowska-Zielinska
beata@fizyka.umk.pl

1 Institute of Physics, Faculty of Physics, Astronomy and Informatics, Nicolaus Copernicus University in Torun, Grudziadzka 5/7, 87-100 Torun, Poland

2 Faculty of Chemistry, Nicolaus Copernicus University in Torun, Gagarina 7, 87-100 Torun, Poland

3 Institute of Mathematics and Physics, Bydgoszcz University of Science and Technology, S. Kaliskiego 7, 85-796 Bydgoszcz, Poland

4 Centre for Modern Interdisciplinary Technologies, Nicolaus Copernicus University, Wilenska 4, 87-100 Torun, Poland

5 Department of Physics, Cracow University of Technology, Podchorążych 1, 30-084 Kraków, Poland

6 University of Lyon, INSA Lyon, UMR5270, ECL, CNRS, UCBL, CPE Lyon, INL, 69621 Villeurbanne, France

Dalasinski et al. 2006; Duvenhage et al. 2015). Alq_3 is a metal chelate that is commonly used as an electron transport layer in organic light-emitting diodes (OLEDs) (Cuba and Muralidharan 2014a). Tang and Van Slyke in 1987 described the use of this material in OLED for the first time (Tang and Slyke 1987), and interest in Alq_3 has been growing ever since. In contrast, the hole transport properties of Alq_3 were investigated by Fong and So (Fong and So 2006).

In our previous research (Derkowska-Zielinska 2017) we have shown that Alq_3 has two main absorption bands (called A and B), which are ligand-centered electronic transitions. The A band (visible in the spectral range of 350–450 nm) is associated with the transition from the ground state to the excited one and is also assigned to charge transfer (CT) from the quinolate ring containing oxygen to the pyridyl ring. It corresponds to the π–π* transition of the qH^{2+}. Therefore, it is attributed to the excitation of π–π* by the molecular orbitals of quinolinate ligands. Whereas B band, which absorption is located in the spectral range of 210–280 nm, suggests the presence of a p-band associated with the central metal atoms, where the transition p–π* is more prominent. It means that the electronic transitions from 3p electronic orbitals to π* molecular orbitals are allowed (Derkowska-Zielinska 2017). Alq_3 is a green emitter with photoluminescence observed in the range of 520 nm. Its emission occurs due to the transition from the highest occupied molecular orbit (HOMO), lying mainly on the phenoxide ring, to the lowest unoccupied molecular orbit (LUMO) located on the pyridyl ring (Lessmann and Hummelgen 2004). In Alq_3, the optical transition responsible for PL is centred on the organic ligand, and the luminescent properties of this compound are mainly associated with the metal (Al)–nitrogen bond (Halls and Schlegel 2001).

Zinc oxide (ZnO) is a promising inorganic semiconductor material. Due to its excellent optical and electrical properties, it has the potential applications in light emitting diodes (LEDs), ultraviolet lasers, photodetectors and piezoelectric devices (Sypniewska et al. 2020). ZnO is n-type metal oxide semiconductor, which has a direct band gap (~ 3.37 eV at RT), large exciton binding energy (60 meV), high electron mobility and high optical transmittance (Sypniewska et al. 2020; Abed et al. 2015; Kapustianyk et al. 2007; Sofiani et al. 2007).

A polymeric material with unique properties, such as light weight, high flexibility and the possibility of production at low temperature and at low-cost, can be used to improve the quality of the thin composite layer (Dorranian et al. 2009). One of the most commonly used polymeric material is poly(methyl methacrylate) (PMMA). Its main advantages are excellent mechanical properties, high chemical resistance, simple synthesis, low-cost, good tensile strength, low optical loss in visible spectral range, good insulation properties and thermal stability. PMMA is considered to be an excellent matrix material due to its good transparency (Suhailath et al. 2017; Derkowska-Zielinska et al. 2016; Ismail et al. 2012). The use of this polymer with Alq_3 was described by Ke-Qin et al. (Ke-Qin et al. 2008), as well as by Mahakhode et al. (Mahakhode et al. 2011). In both studies, the authors observed a blueshift in the luminescence of Alq_3 dispersed in PMMA matrix compared to pure Alq_3 film. The second polymer matrix used in this study was polyvinylpyrrolidone (PVP), which is attractive due to the strong affinity of the pyridine group and its ability to form a hydrogen bond with polar species (Kumar and Buddhudu 2014). Due to the fact that it binds very well with polar particles, it is used in coatings for photo-quality ink-jet papers (Aboud et al. 2009). The formation of transition metal particles inside the polymer system is of interest for some potential applications, such as laser systems, optical lenses and optical planar waveguides (Rzayev et al. 2008). The PVP polymer film has the ability to store charges in response to dopant-dependent optical properties and has a strong tendency to complex with various molecules (Sivaiah et al. 2010).

To develop a new hybrid organic–inorganic structures, which can be used in the production of novel OLED devices, we have prepared thin films containing ZnO, Alq_3 and ZnO:Alq_3 in polymer matrix (PVP or PMMA) by a dip-coating method. Prepared samples were characterized with AFM, SEM, EDX, FTIR spectroscopy, SE and PL. In this studies, we investigated which of the used polymers permits to create more homogeneous and uniform layers, and above all, how (and if) homogeneously Alq_3 and ZnO are embedded in these matrices.

Experimental

Materials

Alq_3, PMMA and PVP (M_w ~ 40 000 g/mol) powders were purchased from Sigma-Aldrich. PMMA was dissolved in tetrahydrofuran (THF) for 7 days forming a 0.2% solution. The 5% PVP solution was obtained by adding polymer powder to isopropanol (Chempur, pure p.a.) and mixed in an ultrasonic cleaner for 30 min.

To obtain the Alq_3 solution with the polymer, 0.02 g of tris(8-quinolinolato)aluminium powder was added to the previously prepared polymer solutions (10 mL) and placed in an ultrasonic bath for approximately 30 min. In the case of Alq_3:PVP layers, the solution was left still for 24 h before deposition.

To obtain a ZnO:Alq_3:polymer suspension, 5 mg of ZnO powder was added to the Alq_3:polymer solutions (10 mL). Then, the Alq_3:polymer solution with added ZnO powder was placed in an ultrasonic bath for 30 min. ZnO powder was prepared using the sol–gel method described in detail

elsewhere (Sypniewska et al. 2020) and annealed from the obtained sol at 500 °C. It should be mentioned that to prepare the sol solution, the zinc acetate dihydrate (Merck) and monoethanolamine (MEA, Sigma-Aldrich, 99.5%) were added to isopropanol alcohol (Chempur, pure p.a.). The sol solution was then heated to 70 °C with continuous stirring and maintained at this temperature for 60 min (Sypniewska et al. 2020).

Thin films preparation

Thin films of polymers, ZnO:polymers, Alq_3:polymers and ZnO:Alq_3:polymers were deposited on a p-Si (100) substrate by dip-coating method (Qualtech QPI-168, Denver, CO, USA) at a substrate withdrawal speed equal of 10 mm/min. The obtained layers were dried at room temperature in an ambient atmosphere for 24 h. The thickness of the thin layers was about 100 nm (the exact values are given in Table 2).

Measurement methods and equipments

The FTIR spectra were measured using FT-IR Vertex 70 V with a Hyperion 1000/2000 microscope by Bruker Optik from 400 cm^{-1} to 4000 cm^{-1}. The luminescent properties of prepared thin layers on Si substrates were registered by the spectrometer FP-8200 in the range of 2.1–3.4 eV ($\lambda_{ex.} = 325$ nm, Xe lamp). The refractive indices (n) and extinction coefficients (k) were determined by the ellipsometric method using the V-VASE spectroscopic ellipsometer (J. A. Woollam Co., Inc.) (Skowronski et al. 2015). The ellipsometric azimuths Ψ and Δ were recorded at the different three angles of incidence (65°, 70° and 75°). The dispersion properties of extinction coefficient (k) and refractive index (n) were parameterized using Gaussian oscillators and Tauc–Lorentz oscillators (for ZnO:polymer layers). The analysis of the surface topography of the studied films was performed using Atomic Force Microscopy (AFM, Veeco microscope, Plainview, NY, USA) with the following scan parameters: size 5 × 5 μm^2 with the scan rate of 1 Hz in the tapping mode. The mean surface roughness i.e. the average roughness $\left(R_a = \frac{1}{N}\sum_{i=0}^{N}|y_i|\right)$ and the root mean square roughness $\left(R_q = \sqrt{\frac{1}{N}\sum_{i=0}^{N}y_i^2}\right)$ were determined using the NanoScope Analysis software. The quantities y_i and N used in R_a and R_q are the current surface height value and number of measured points, respectively. Scanning electron microscopy (SEM) studies were performed with a Quanta 3D FEG (FEI, Hillsboro, OR, USA) (EHT = 30 kV) instrument. Energy Dispersive X-ray spectroscopy (EDX) studies were performed with a Quantax 200 with XFlash 4010 detector by Bruker AXS (Germany).

Results and discussion

Thin films of pure polymers PVP and PMMA, Alq_3:polymer (PVP or PMMA), ZnO:polymer (PVP or PMMA) and ZnO:Alq_3:polymer (PVP or PMMA) composites were deposited on silicon substrates by dip-coating method. Isopropanol and tetrahydrofuran (THF) were used as solvents. It was found that isopropanol is a good solvent for PVP and Alq_3, while THF (Bistac and Schultz 1997) was more suitable for PMMA and Alq_3 samples preparation. It should be noted that dip-coating method used for the production of thin films is not only a simple technique, but also very useful for creating smooth layers of composite materials (Cuba and Muralidharan 2014a; Szczesny et al. 2016).

FTIR spectra measured for thin films of pure polymers, Alq_3:polymer (PVP or PMMA), ZnO:polymer (PVP or PMMA) and ZnO:Alq_3:polymer (PVP or PMMA) composites are presented in Fig. 1. The peak positions and the assigned vibration modes are summarized in Table 1.

The characteristic vibration mode for pure Alq_3 layers are: a wide band observed around 3414 cm^{-1} (caused by characteristic OH stretching vibrations), a band at 3047 cm^{-1} (attributed to (C–H) stretching vibrations in the Alq_3 aromatic ring), a band at 1601 cm^{-1} (C=C), bands at 1582 cm^{-1}, 1491 cm^{-1} and 1425 cm^{-1} (result from the conjugated action of aromatic rings in the Alq_3 molecule), bands at 1370–1250 cm^{-1} (C–N–C bond), band at 758 cm^{-1} (Al–O–Al), bands at 557–644 cm^{-1} (Al–O) and band at

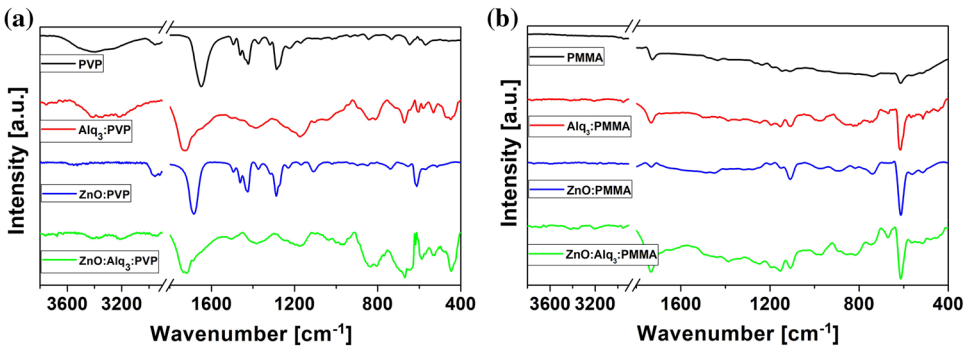

Fig. 1 FTIR spectra of thin layers of **a** pure PVP, Alq_3:PVP, ZnO:PVP and ZnO:Alq_3:PVP; **b** pure PMMA, Alq_3:PMMA, ZnO:PMMA and ZnO:Alq_3:PMMA

Table 1 Peak positions and the assigned vibration modes for polymers and Alq_3, ZnO and ZnO:Alq_3 thin layers in polymer matrices: PVP and PMMA (pp—peak position, vm—vibration mode)

PVP		Alq_3:PVP		ZnO:PVP		ZnO:Alq_3:PVP	
pp [cm^{-1}]	vm	pp [cm^{-1}]	vm	pp [cm^{-1}]	vm	pp [cm^{-1}]	vm
735	$\rho(CH_2)$	445	ν(Al–N)	512	ν_s(Zn–O)	436	ν(Al–N)
958	ν(C–O)	557;604;678	ν_s(Al–O)	738	$\rho(CH_2)$	457	ν_s(Al–O)
996	$\omega(CH_2)$	585	δ(N–C=O)	1104	$\tau(CH_2)$	520	ν_s(Zn–O)
1097	$\tau(CH_2)$	743	ν_s(Al–O–Al)	1163	ν(C–O–C)	585	δ(N–C=O)
1172	ν(C–O–C)	813–836	$\delta(CH_2)$	1287	ν(C–O)	781	ν_s(Al–O–Al)
1277	ν(C–O)	1032	δ(C–C)	1372	$\tau(CH_2)$	958	δ(C–C)
1377	$\tau(CH_2)$	1368	δ(C–H)	1687	ν(C=O)	1023	δ(C–C)
1732	ν(C=O)	3100–3600	ν(OH)	3000–2800	δ(C–H)	1163	ν_s(C–OH)
2924	δ_{as}(C–H)					1368	δ(C–H)
2943	δ_{as}(C–H)					1730	ν(C=O)
						2933	$\nu(CH_2)$
						3200–3600	ν(OH)
PMMA		Alq_3:PMMA		ZnO:PMMA		ZnO:Alq_3:PMMA	
pp [cm^{-1}]	vm	pp [cm^{-1}]	vm	pp [cm^{-1}]	vm	pp [cm^{-1}]	vm
750	δ(C–C)	426	ν(Al–N)	512	ν_s(Zn–O)	463	ν(Al–N)
836	$\nu(CH_2)$	613	ν_s(Al–O)	738	$\rho(CH_2)$	510	ν_s(Zn–O)
986	$\delta(O–CH_3)$	750	δ(C–C)	816	$\nu(CH_2)$	557–604	ν_s(Al–O)
1144	ν(C–O–C)	752	ν_s(Al–O–Al)	970	$\delta(O–CH_3)$	752	δ(C–C)
1237	ν(C–O–C)	827	$\nu(CH_2)$	1150	ν(C–O–C)	790	ν_s(Al–O–Al)
1433	δ(C–H)	995	$\delta(O–CH_3)$	1279	ν(C=O)	980	$\delta(O–CH_3)$
1489	$\nu(CH_2)$	1140	ν(C–O–C)	1448	$\nu(CH_2)$	1107	ν(C–OH)
1635	ν(C=O)	1218	ν(C–O–C)	1726	ν(C=O)	1144	ν(C–O–C)
1712	ν(C=O)	1256	ν_s(C–N–C)			1247	ν_s(C–N–C)
2853	δ(C–H)	1489	δ(C–H)			1386	δ(C–H)
2961	δ(C–H)	1732	ν(C=O)			1741	ν(C=O)
3000	δ(C–H)	2952	δ(C–H)			2961	δ(C–H)
		3100–3600	ν(OH)			3200	ν(OH)

about 460 cm^{-1} (Al–N) (Cuba and Muralidharan 2014b). Typical bands for ZnO annealed at 500 °C are presented in Ref. (Sypniewska et al. 2020). From Fig. 1 and Table 1, we can see that in the FTIR spectrum of ZnO:Alq_3:polymer thin film exists a contribution coming from the polymer matrix and the corresponding Alq_3 and ZnO bands. FTIR measurements thus confirm the presence of all constituent composites.

Figure 2 shows the topographic images for all studied samples obtained by the Atomic Force Microscopy, while Table 2 presents the calculated roughness parameters R_q and R_a (see also subsection 2.3).

For the pure polymers, the parameter R_a is in the range of 1.3–2.5 nm, and R_q takes the values 1.8–3 nm. After adding Alq_3 and ZnO to the polymer matrices, a substantial increase in the R_a and R_q parameters is observed. In the case of ZnO:Alq_3 in PVP thin films, the island shape was scattered. Similar behavior was found by Kim et al. (2019). However, their obtained R_q value for the PVP–ZnO thin layer is 5.0 nm, which is slightly lower compared to our film.

The morphology of the investigated thin layers is shown in Fig. 3. These SEM images confirm that we obtained smooth layers for the PVP and PMMA polymers (see Fig. 3a, b). ZnO particles visible in Fig. 3h are unevenly distributed on the surface of the samples. We found that for ZnO:polymer and ZnO:Alq_3:polymer samples, the ZnO crystallite size is the largest for the PMMA polymer. The ZnO agglomerates in the PMMA polymer have a lateral size of about 2–3 µm. This is not evident in the PVP polymer as this polymer prevents the formation of agglomerates (Koczkur et al. 2015). SEM micrographs for Alq_3:PMMA and ZnO:Alq_3:PMMA show Alq_3 agglomerates with elongated shape, which are not noticeable in the case of the PVP polymer.

EDX mapping analysis of ZnO:Alq_3:PVP and ZnO:Alq_3:PMMA are shown in Fig. 4. It should be mentioned that the EDX analysis complements the SEM and AFM studies. From these mapping, we can see how the individual particles containing Zn and Al in their composition are distributed on the sample surface. EDX shows that agglomerates containing Zn and Al are formed for the sample with the PMMA polymer, which is not observed for the PVP polymer matrix.

Spectroscopic ellipsometry (SE) allows determining the optical constants, such as the refractive index (n) and the extinction coefficient (k). These constants were determined

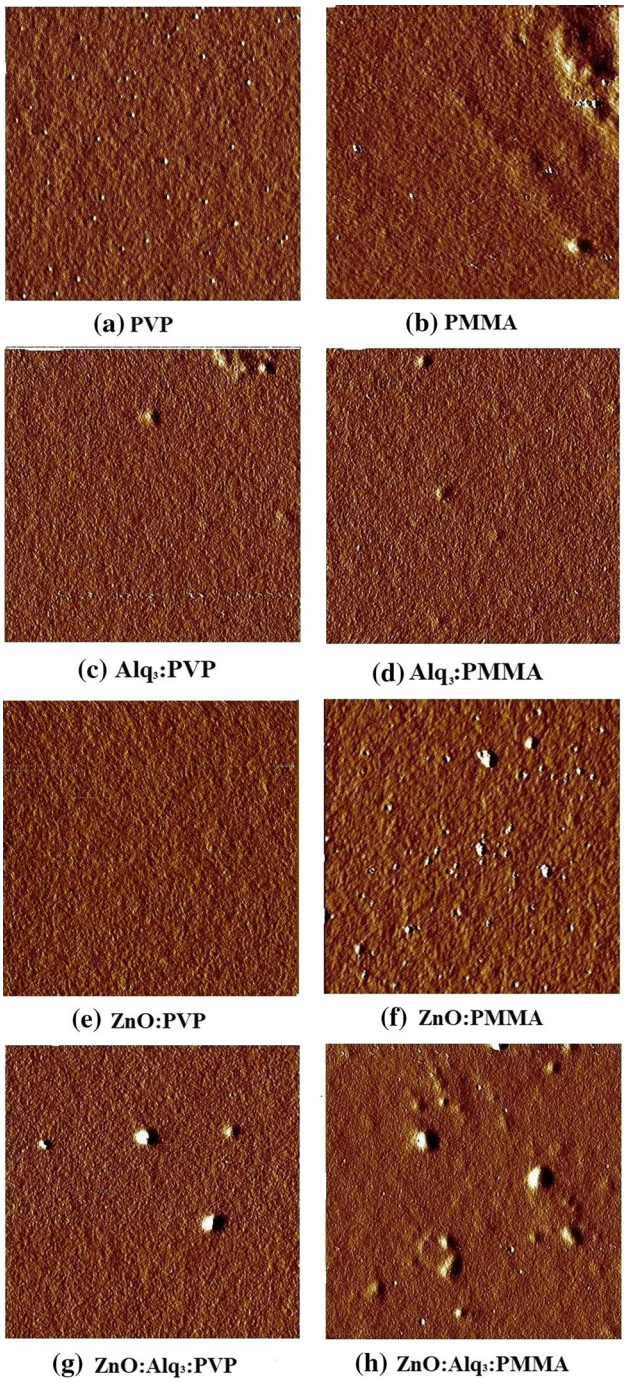

Fig. 2 Surface topography obtained from AFM (5×5 μm^2) of: pure polymers **a** PVP, **b** PMMA, respectively; Alq_3 in the polymer matrix of: **c** PVP, **d** PMMA, respectively; ZnO in the polymer matrix of: **e** PVP, **f** PMMA, respectively; ZnO:Alq_3 in the polymer matrix of: **g** PVP, **h** PMMA

using the silicon/silicon oxide/Alq_3:polymer layer/rough layer/ambient or silicon/silicon oxide/ZnO:Alq_3:polymer layer/rough layer/ambient optical model of the sample. We used the Gaussian and Tauc–Lorentz oscillators (for ZnO:polymer layers) to parametrize the dispersion properties of n and k.

Table 2 Values of roughness parameters R_q and R_a, as well as the values of a thickness (d) and optical energy band gap (E_g)

Sample	R_q [nm]	R_a [nm]	d [nm]	E_g [eV]
PVP	3.0	2.5	–	–
Alq_3:PVP	8.7	7.5	116 ± 1	2.74 ± 0.02
ZnO:PVP	8.9	8.5	135 ± 1	5.14 ± 0.04
ZnO:Alq_3:PVP	8.8	12.0	110 ± 1	2.79 ± 0.02
PMMA	1.8	1.3	–	–
Alq_3:PMMA	2.7	2.9	102 ± 1	2.99 ± 0.02
ZnO:PMMA	4.0	2.0	84 ± 1	4.45 ± 0.02
ZnO:Alq_3:PMMA	10.8	8.6	114 ± 1	3.13 ± 0.03

Figure 5 presents the refractive index (n) as a function of photon energy for all studied thin films. One can see that the refractive index exhibits normal dispersion in the spectral range up to 3.0–3.2 eV, and it shows anomalous dispersion at energies above 3.2 eV. Plots for ZnO:polymer show the shapes typical of PVP and PMMA polymers due to insufficient number of ZnO particles on the sample surface. In addition, we can notice that the values of the refractive index of ZnO:Alq_3:PVP and ZnO:Alq_3:PMMA are higher compared to Alq_3:PVP, Alq_3:PMMA, ZnO:PVP and ZnO:PMMA in normal dispersion region. We also found that the n values for Alq_3:PVP, ZnO:PVP and ZnO:Alq_3:PVP are higher compared to studied materials in PMMA matrix. Similar shapes of refractive index are obtained for Alq_3:PVP and Alq_3:PMMA, as well as for ZnO:Alq_3:PVP and ZnO:Alq_3:PMMA.

Figure 6 shows the extinction coefficient (k) as a function of the photon energy for studied samples. In the spectra for two-component thin layers, Alq_3:polymers, three bands are observed: two strong ones in the ranges of 2.3–3.7 eV and 4.3–5.2 eV and weak bands in the range of 3.7–4.3 eV. Band in region of 2.3–3.7 eV (called A band) is connected with a transition from a ground state to an excited state and is attributed to the π–π* excitation involving molecular orbitals of the quinolinate ligands. The location of the second band 4.3–5.2 eV (B band) suggests the presence of a p-band associated with the central metal atoms, where the transition p–π* is more prominent. Weak bands in the range of 3.7–4.3 eV (called C and D bands) are identified with vibronic progression due to the deformation mode of the electron transition ring. These bands can be attributed to different electronic transitions than the main strong bands.

From Fig. 6, we can also see a redshift of only A band (i.e. from 3.1 to 3.3 eV) for Alq_3:PVP compared to Alq_3:PMMA. For samples ZnO:Alq_3:polymer we observe only two main bands 2.2–4.3 eV and 4.3–5.3 eV. In addition, we can observe the redshift of extinction coefficient

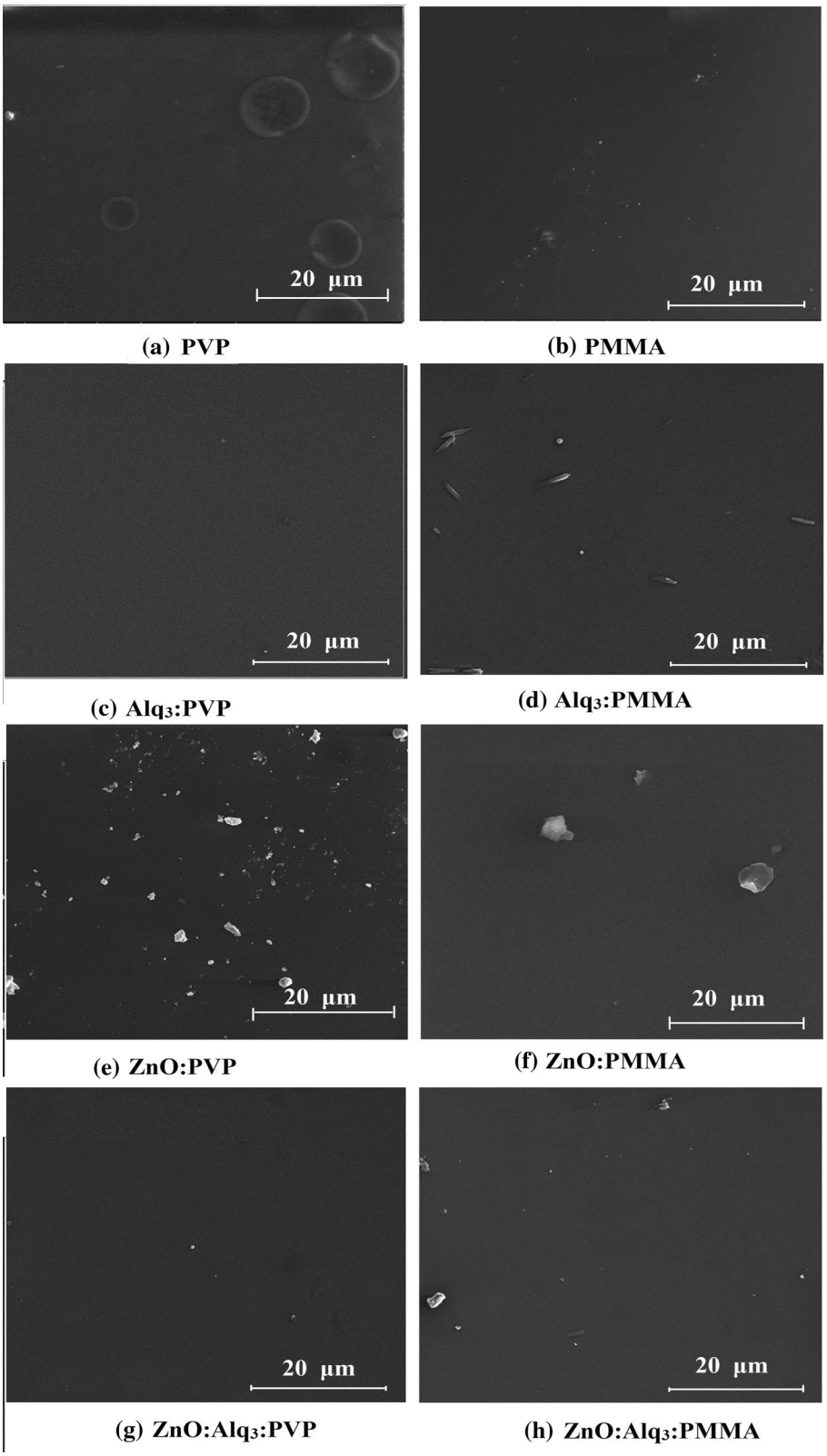

Fig. 3 SEM micrographs of thin films of: pure polymers **a** PVP, **b** PMMA, respectively; Alq_3 in the polymer matrix of: **c** PVP, **d** PMMA, respectively; ZnO in the polymer matrix of **e** PVP, **f** PMMA, respectively; ZnO:Alq_3 in the polymer matrix of: **g** PVP, **h** PMMA, respectively

of ZnO:Alq_3:PVP compared to ZnO:Alq_3:PMMA. In addition, in the case of ZnO:Alq_3:PMMA, an additional band at 5.2 eV can be seen due to visible band in Alq_3:PMMA.

Figure 7 presents the Tauc plots of the studied thin films as a function of photon energy with the extrapolation of the linear part of the $(\alpha h\nu)^2$ relation (where α is

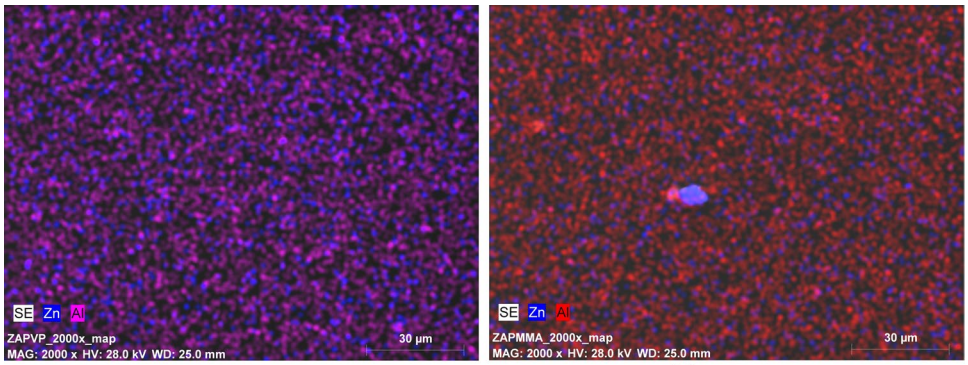

(a) ZnO:Alq_3:PVP **(b)** ZnO:Alq_3:PMMA

Fig. 4 EDX mapping analysis images for **a** ZnO:Alq_3:PVP and **b** ZnO:Alq_3:PMMA thin films. The Zn particles are blue and Al are purple for the ZnO:Alq_3:PVP sample (**a**) for the ZnO:Alq_3:PMMA sample, Zn particles are also blue, while Al-containing areas are red (**b**)

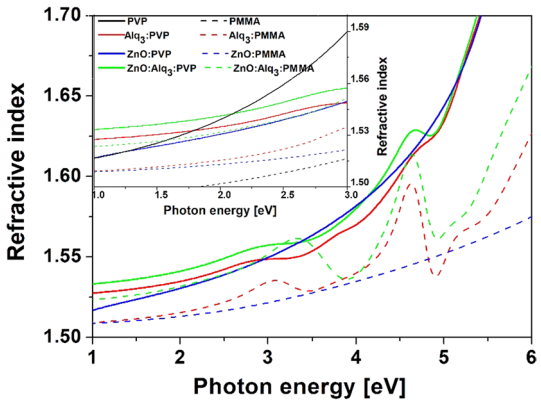

Fig. 5 Refractive index (n) versus photon energy for thin films Alq_3, ZnO and ZnO:Alq_3 in PVP and PMMA polymer matrix, respectively

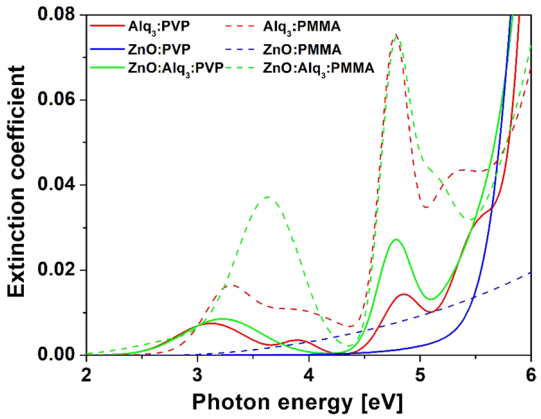

Fig. 6 Extinction coefficient versus photon energy for thin films Alq_3, ZnO and ZnO:Alq_3 in PVP and PMMA matrix

absorption coefficient calculated from $\alpha = \frac{4\pi k}{\lambda}$). The determined values of optical energy band gap (E_g) are shown in Table 2. Prepared thin layers of Alq_3 in a polymer matrix were found to exhibit the energy gap of 2.74 eV for PVP and 2.99 eV for PMMA. These values are similar to those reported by Cuba et al. (Cuba and Muralidharan 2014b), i.e. $E_g = 2.87$ eV for Alq_3 film prepared by dip-coating method. For ZnO:Alq_3:polymer thin layers, the energy gap were determined as 2.79 eV for the PVP polymer matrix, and 3.13 eV for the PMMA polymer. Increasing the optical energy gap has the effect of shifting the absorption threshold toward the shorter wavelengths, along with the decreasing particle size. This relationship is called the quantum size effect. It also leads to an increase in the molar absorption coefficient, which is related to the overlapping of the wave functions of the charge carriers (Trindade et al. 2001). We found that the values of E_g are 5.14 eV and 4.45 eV for the ZnO:PVP and ZnO:PMMA, respectively. These values are approximate for the literature values of energy band gaps in the range given by Baskoutas et al. (~5–7 eV) for the PVP polymer (Vempati et al. 2013; Baskoutas and Terzis 2006) and 4.9 eV for PMMA (Aziz et al. 2017).

Figure 8 shows the photoluminescence spectra for thin films of pure PVP and PMMA, Alq_3:polymer (PVP or PMMA), ZnO:polymer (PVP or PMMA) and ZnO:Alq_3:polymer (PVP or PMMA), which were obtained using an excitation wavelength of 325 nm at room temperature.

A typical Alq_3 luminescence spectrum is characterized by a single broad peak in the range of 2.13–2.75 eV with a maximum at ca. 2.38 eV (Cuba and Muralidharan 2014a). On the other hand, PL spectrum of ZnO layer demonstrates two bands: a strong emission band focused around 3.26 eV due to the emission of a free exciton and second band at 2.58 eV to 1.55 eV (yellow–orange emission) (Sypniewska et al. 2020). In the case of Alq_3:polymer (PVP or PMMA) samples, it can be supposed that the final luminescence spectrum is the combination of the typical spectrum of the Alq_3 and the one of the pure polymer. The addition of polymer to Alq_3 caused the luminescence maximum to shift toward higher energies, 2.46 eV for PVP and 2.45 eV for PMMA. After the addition of ZnO, the maxima for the three-component layers were not changed. In the case of the ternary

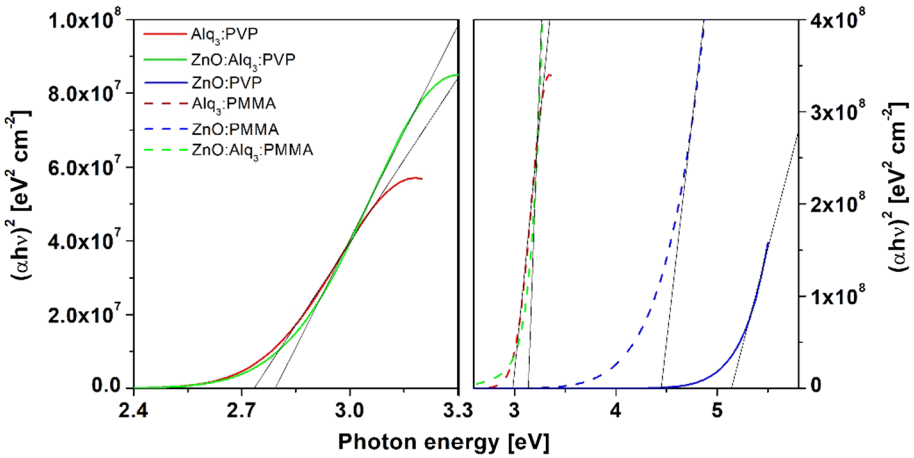

Fig. 7 Tauc plots of the studied thin films

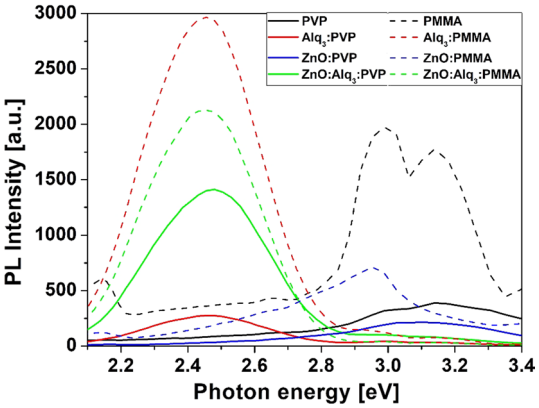

Fig. 8 PL spectra for PVP, PMMA, as well as Alq_3, ZnO and ZnO:Alq_3 in PVP and PMMA polymer matrix, respectively

samples for PVP polymers, an increase in the intensity of luminescence can be noticed compared to the samples with Alq_3 alone. Such enhancement may result from compatible energy levels of the organic and inorganic material. They can also be attributed to the distortion caused by the incorporation of ZnO over the Alq_3 molecules (Cuba and Muralidharan 2014b).

Conclusions

The main object of the present work was to develop a new hybrid organic–inorganic structure, which can be used in the production of innovative OLED devices.

The AFM and SEM measurements show that relatively smooth layers were obtained for the PVP and PMMA polymers. Thin layers with smooth surfaces of Alq_3, ZnO and ZnO:Alq_3 were also successfully prepared in PVP and PMMA polymer matrices using the dip-coating method. In addition, the sizes of the visible ZnO crystallites in the three-component samples change. The EDX analysis complements the SEM and AFM analyses showing how the individual Zn and Al particles are distributed on the sample surface. Spectroscopic ellipsometry was used to determine the refractive indices and extinction coefficients of the obtained two- and three-component layers. In the spectral range up to 3.0–3.2 eV, refractive index exhibits normal dispersion and in the energy above 3.2 eV it shows anomalous dispersion. For two-component thin layers, Alq_3:polymer (PVP or PMMA), three bands are observed in the extinction coefficient: two strong ones in the ranges of 2.3–3.7 eV and 4.3–5.2 eV and weak bands in the range of 3.7–4.3 eV. For samples ZnO:Alq_3:polymer, we can see two main bands 2.2–4.3 eV and 4.3–5.3 eV. In addition, the optical energy band gaps were determined for the thin layers under study and were equal to 2.74 eV and 2.99 eV for Alq_3:PVP and Alq_3:PMMA, respectively. For the three-component layers, we obtained the E_g values as 2.79 eV for the PVP polymer and 3.13 eV for the PMMA polymer. Measurements of PL of Alq_3 in polymer matrices under 325 nm excitation showed a blue shift in relation to pure Alq_3 layers.

In conclusion, after analysing the produced thin films and examining their optical and structural properties, we found that PVP would be a better polymer for OLED applications.

Acknowledgements M.S., A.A. and B. D.-Z. thank the NAWA PHC Polonium Project (No. BPN/BFR/2021/1/00036) for the financial support.

Declarations

Conflict of interest There is no conflict of interest.

References

Abed S, Bougharraf H, Bouchouit K, Sofiani Z, Derkowska-Zielinska B, Aida MS, Sahraoui B (2015) Influence of concentration of nano particles of Bi on the electrical and optical properties of ZnO thin films. Superlattices Microstruct 85:370–378. https://doi.org/10.1016/j.spmi.2015.06.008

Aboud SR, Kareem A, Al-Bermany J, Megahed N (2009) Effect of Temperature on Some Rheological Properties of Polyvinyl Pyrrolidone (PVP). Egypt J Solids 32:81–88. https://doi.org/10.21608/EJS.2009.148779

Aziz SB, Abdullah OG, Hussein AM, Ahmed HM (2017) From Insulating PMMA polymer to conjugated double bond behavior: green chemistry as a novel approach to fabricate small band gap polymers. Polymers 9(11):1–15. https://doi.org/10.3390/polym9110626

Baskoutas S, Terzis AF (2006) Size-Dependent Band Gap of Colloidal Quantum Dots. J Appl Phys 99(1):013708. https://doi.org/10.1063/1.2158502

Bistac S, Schultz J (1997) Study of solution-cast films of PMMA by dielectric spectroscopy: influence of the nature of the solvent on and/ relaxations. Int J Adhesion Adhesives 17:197–201. https://doi.org/10.1016/S0143-7496(97)00001-8

Boeckler C, Feldhoff A, Oekermann T (2007) Electrodeposited Zinc Oxide/Phthalocyanine Films – An Inorganic/ Organic Hybrid System with Highly Variable Composition. Adv Funct Mater 17:3864–3869. https://doi.org/10.1002/adfm.200700619

Coe S, Woo WK, Bawendi M, Bulovic V (2002) Electroluminescence from single monolayers of nanocrystals in molecular organic devices. Nature 420:800–803. https://doi.org/10.1038/nature01217

Cuba M, Muralidharan G (2014a) Effect of thermal annealing on the structural and optical properties of tris-(8-hydroxyquinoline) aluminum(III) (Alq_3) films. Luminescence 30:1–6. https://doi.org/10.1002/bio.2738

Cuba M, Muralidharan G (2014b) Enhanced luminescence properties of hybrid Alq_3/ZnO (organic/inorganic) composite films. J Lumin 156:1–7. https://doi.org/10.1016/j.jlumin.2014.07.008

Dalasinski P, Łukasiak Z, Rebarz M, Wojdyła M, Bała W (2006) Study of optical properties of TRIS (8-hydroxyquinoline) aluminum (III). Opt Mat 28:98–101. https://doi.org/10.1016/j.optmat.2004.10.031

Derkowska-Zielinska B (2017) Enhancement of third order nonlinear optical susceptibility of Alq_3 in polar aprotic solvents. Opt Lett 42:567–570. https://doi.org/10.1364/OL.42.000567

Derkowska-Zielinska B, Krupka O, Smokal V, Grabowski A, Naparty M, Skowronski L (2016) Optical properties of disperse dyes doped poly(methyl methacrylate). Mol Cryst Liq Crystals 639:87–93. https://doi.org/10.1080/15421406.2016.1254585

Dorranian D, Abedini Z, Hojabri A, Ghoranneviss M (2009) Structural and optical characterization of PMMA surface treated in low power nitrogen and oxygen RF plasmas. J Non-Oxide Glasses 1:217–229

Duvenhage MM, Ntwaeaborwa OM, Swart HC (2015) Optical and chemical properties of Alq_3:PMMA blended thin films. Mater Today Proc 2:4019–4027. https://doi.org/10.1016/j.matpr.2015.08.031

Fong HH, So SK (2006) Hole transporting properties of tris(8-hydroxyquinoline) aluminum (Alq_3). J App Phys 100:1–5. https://doi.org/10.1063/1.2372388

Halls MD, Schlegel BH (2001) Molecular Orbital Study of the First Excited State of the OLED Material Tris(8-hydroxyquinoline) aluminum(III). Chem Mater 13:2632–2640. https://doi.org/10.1021/cm010121d

Ismail LN, Zulkefle H, Herman SH, Mahmood MR (2012) Influence of Doping Concentration on Dielectric, Optical, and Morphological Properties of PMMA Thin Films. Adv Mater Sci Eng 2012:1–5. https://doi.org/10.1155/2012/605673

Kapustianyk V, Turko B, Kostruba A, Sofiani Z, Derkowska B, Dabos-Seignon S, Barwiński B, Eliyashevskyi Yu, Sahraoui B (2007) Influence of size effect and sputtering conditions on the crystallinity and optical properties of ZnO thin films. Opt Commun 269:346–350. https://doi.org/10.1016/j.optcom.2006.08.034

Ke-Qin T, Chun-Xian X, Qiong W, Bao-Xiang G, Ke Z, Li-Hua Y, Xin-Song L (2008) Photoluminescence of Electrospun Poly-Methyl-Methacrylate:Alq_3 Composite Fibres. Chin Phys Lett 25:4453–4455. https://doi.org/10.1088/0256-307X/25/12/075

Kim O, Kwon JB, Kim SW, Xu B, Seo KH, Park CE, Do WJ, Bae JH, Kang S (2019) Effect of PVP- capped ZnO nanoparticles with enhance charge transport on the performance of P3HT/PCBM polymer solar cells. Polymers 11:3–10. https://doi.org/10.3390/polym11111818

Koczkur KM, Mourdikoudis S, Polavarapu L, Skrabalak SE (2015) Polyvinylpyrrolidone (PVP) in nanoparticle synthesis. Dalton Trans R Soc Chem 44:17883–17905. https://doi.org/10.1039/C5DT02964C

Kumar KN, Buddhudu S (2014) Enhanced photoluminescence of Mn^{2+}+Tb^{3+}Ions doped PEO+PVP blended polymer films. Proc Indian Nat Sci Acad 80:345–354. https://doi.org/10.16943/ptinsa/2014/v80i2/55112

Lessmann R, Hummelgen IA (2004) Thin copolymer-cased light-emitting display made with fluorine-foped tin oxide substrates. Mater Res 7:467–471. https://doi.org/10.1590/S1516-14392004000300015

Mahakhode JG, Dhoble SJ, Joshi CP, Moharil SV (2011) Blue-shifted photoluminescence of Alq_3 dispersed in PMMA. Bull Mater Sci 34:1649–1651. https://doi.org/10.1007/s12034-011-0372-1

Onlaor K, Tunhoo B, Thiwawong T, Nukeawa J (2012) Electrical bistability of tris-(8- hydroxyquinoline) aluminum (Alq_3)/ZnSe organic-inorganic bistable device. Curr Appl Phys 12:331–336. https://doi.org/10.1016/j.cap.2011.07.004

Rzayev ZMO, Denizli BK, Denizli H (2008) Bioengineering functional Copolymers. XI. Copper (11)-Poly (N-vinyl-2-pyrrolidone-N-isopropylacrylamide) macro complexes. J Appl Polym Sci 109:903–909. https://doi.org/10.1002/app.26329

Sanchez C, Belleville BJP, Popall M (2005) Applications of hybrid organic–inorganic nanocomposites. J Mater Chem 15:3559–3592. https://doi.org/10.1039/B509097K

Sivaiah K, Rudramadevi B, Buddhudu S, Kumar G (2010) Structural, thermal and optical properties of Cu2+ and Co2+: PVP polymer films. Indian J Pure Appl Phys 48:658–662

Skowronski L, Krupka O, Smokal V, Grabowski A, Naparty M, Derkowska-Zielinska B (2015) Optical properties of coumarins containing copolymers. Opt Mat 47:18–23. https://doi.org/10.1016/j.optmat.2015.06.047

Sofiani Z, Sahraoui B, Addou M, Adhiri R, Alaoui M, Dghoughi L, Fellahi N, Derkowska B, Bala W (2007) Third harmonic generation in undoped and X doped ZnO films (X: Ce, F, Er, Al, Sn) deposited by Spray Pyrolysis. J Appl Phys 101:1–5. https://doi.org/10.1063/1.2711143

Suhailath K, Ramesan MT, Naufal B, Periyat P, Jasna VC, Jayakrishnan P (2017) Synthesis, characterisation and flame, thermal and electrical properties of poly (n-butyl methacrylate)/titanium dioxide nanocomposites. Polym Bull 74:671–688. https://doi.org/10.1007/s00289-016-1737-9

Sypniewska M, Szczesny R, Popielarski P, Strzałkowski K, Derkowska-Zielinska B (2020) Structural, morphological and photoluminescent properties of annealed ZnO thin layers obtained by the rapid sol-gel spin-coating method. Opto-Electron Rev 28:182–190. https://doi.org/10.24425/opelre.2020.134460

Szczesny R, Szlyk E, Wisniewski MA, Hoang TK, Gregory DH (2016) Facile preparation of copper nitride powders and nanostructured films. J Mater Chem C 4:5031–5037. https://doi.org/10.1039/C6TC00493H

Tang CW, Van Slyke SA (1987) Organic electroluminescent diodes. Appl Phys Lett 51:913–915. https://doi.org/10.1063/1.98799

Trindade T, O'Brien P, Pickett NL (2001) Nanocrystalline semiconductors: synthesis, properties, and perspectives. Chem Mat 13:3843–3858. https://doi.org/10.1021/cm000843p

Vempati S, Ertas Y, Uyar T (2013) Sensitive surface states and their passivation mechanism in CdS Quantum Dots. J Phys Chem C 117:21609–21618. https://doi.org/10.1021/jp408160h

Yoshida T, Zhang J, Komatsu D, Sawatani S, Minoura H, Pauporte T, Lincot D, Oekermann T, Schlettwein D, Tada H, Wohrle D, Funabiki K, Matsui M, Miura H, Yanagi H (2009) Electrodeposition of inorganic/organic hybrid thin films. Adv Funct Mater 19:17–43. https://doi.org/10.1002/adfm.200700188